EPJ Web of Conferences **94**, 02011 (2015)
DOI: 10.1051/epjconf/20159402011

The effect of grain size on dynamic tensile extrusion behaviour

Leeju Park[a], Hack Jun Kim, and Seok Bong Kim

Agency for Defense Development, PO Box 35-42, Taejon 305-600, Korea

Abstract. Dynamic tensile extrusion (DTE) tests were conducted on coarse grained and ultrafine grained (UFG) OFHC Cu, Interstitial free (IF) Steel, and pure Ta. Equal channel angular pressing (ECAP) of 16passes with Bc for Cu, IF Steel and 4 passes for Ta was employed to fabricated UFG materials. DTE tests were carried out by launching the sphere samples (Dia. 7.62 mm) to the conical extrusion die at a speed of ∼500 m/sec. The fragmentation behavior of the soft-recovered fragments were examined and compared with each other. The DTE fragmentation behavior of CG and UFG was numerically simulated by the LS-DYNA FEM code.

1. Introduction

DTE technique is a newly developed mechanical test [1]. In the ordinary DTE test, a spherical sample launched at high velocity passes through an open conical die. Due to the smaller die exit diameter than the sample diameter, the sample experiences severe tensile deformation. Therefore, the DTE test can characterize the mechanical response of materials under both high strain rate and high strain circumstances. The DTE technique has been applied to coarse grained (CG) pure metals such as Cu [1], Ta [2], Zr [3], etc..

Extensive and intensive researches during past two decades clearly reveal that ultrafine grained (UFG) materials exhibit very different mechanical and thermal responses from CG materials. There are several studies on mechanical behavior of UFG materials at high strain rates [4]. However, the strain rate employed in those studies (typically $10^3\ s^{-1}$order) was quite lower than that being attainable in the dynamic tensile extrusion (DTE) test.

Ultrafine grained (UFG) materials usually exhibit higher strength due to the Hall-Petch strengthening but lower ductility due to shear localization than coarse grained (CG) counterparts at room temperature [5]. Meanwhile, some UFG materials show high strain rate super plasticity (HSRS) at high temperatures [6]. The shear localization is beneficial for the self-sharpening of the kinetic energy penetrator. HSRS is possible to operate on the metal jet formation of the metal liner in the chemical energy penetrator [7]. Accordingly, UFG materials are promising as the high performance penetrator materials. In this study, the metal jet formability of UFG OFHC Cu, IF steel and pure Ta were compared to those of CG counterparts by means of DTE test.

2. Experimental

Commercial OFHC annealed Cu and IF steel bars (18 mm diameter) were subjected to 16 passes equal channel angular pressing (ECAP) with route B_c in order to fabricate equiaxed UFG samples. Pure Ta bars were conducted with 4 passes ECAP with route B_c for fabricating UFG samples. The sphere samples of 7.62 mm diameter were machined from the central part of unECAPed and ECAPed bars for DTE tests. DTE tests were carried out by using an all-vacuumed gas gun system which consists of the gas gun, the sample flying barrel, the DTE die chamber, and the sample recovery station; the details of the DTE equipment are described elsewhere [8]. The velocity of sample in this experiment was ∼500 m/sec upon reaching the DTE die. After DTE tests, the sample fragments were soft recovered. The numbers and the order of fragments exiting the die were confirmed by the high speed photography. Besides, the complete fragment recovery was ensured by comparing the weight of all fragments with that of the initial sample. A routine microstructural observation were made on CG and UFG materials before the DTE tests with optical microscopy and electron backscattered diffraction (EBSD). The DTE behavior of CG and UFG Cu was numerically analyzed by using a commercial finite element code (LS-DYNA 2-dimensional axis-symmetric model [9]). The Johnson–Cook model was employed in the numerical analysis. Five unknown parameters in the Johnson–Cook model were obtained by conducting tensile tests at $10^3\ s^{-1}$ and $1\ s^{-1}$ and compression tests at $2000{\sim}4000\ s^{-1}$ on CG and UFG materials; tensile tests and compression tests were carried out on a hydraulic universal testing machine and a split Hopkinson pressure bar tester, respectively. In the numerial simulation process, the 2D R-adaptive remeshing was done in order to prevent severe distortion of the mesh. That is, a completely new mesh was created every 1 μsec in order for the elements to keep a regular shape and a characteristic dimension. The new mesh is initialized from the old mesh by a least square approximation. The simulation results were compared with the experimetal ones in terms of total DTE elongation (sum of the axial elongation of individual fragment) and the number and the dimension of fragments).

[a] Corresponding author: ljparkr@add.re.kr

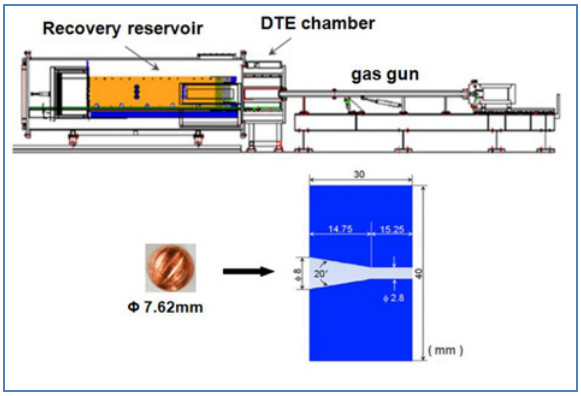

Figure 1. (a) The schematic illustration of the DTE facility consists of gas gun system, (b) Configuration of the DTE die (dimension in mm).

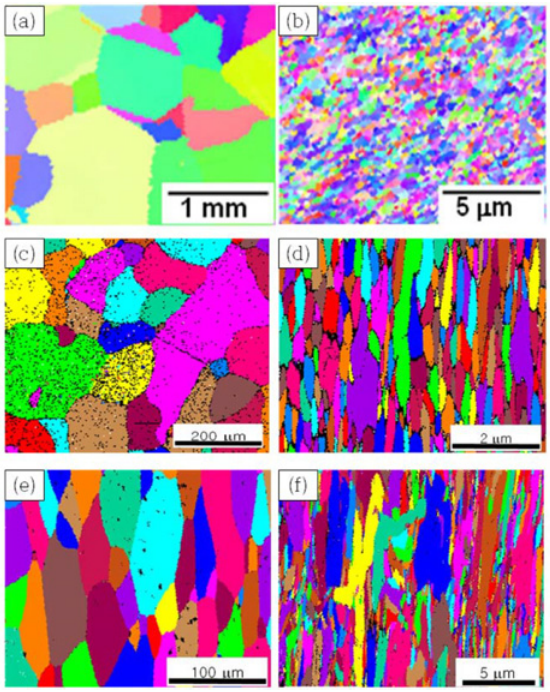

Figure 2. IPF maps (a) CG OFHC Cu, (b) UFG Cu, (c) CG IF Steel, (d) UFG IF Steel, (e) CG Ta, and (f) UFG Ta.

3. Results and discussion

3.1. Examine the grain size of CG and UFG materials

The Inverse pole figure (IPF) maps of the plane parallel to the extrusion axis of the CG and UFG samples are shown in Fig. 2. The average grain size of CG OFHC Cu was ∼1mm and that of UFG Cu was ∼0.35 μm. The average grain size of IF steel was ∼163 μm and that of UFG IF was ∼0.61 μm. The average grain size of CG Ta was ∼53 μm and that of UFG Ta was ∼3.94 μm. IF steel and Ta has a weak texture after ECAP. The grain size difference of CG and UFG samples were range from a few times to 10^6 times.

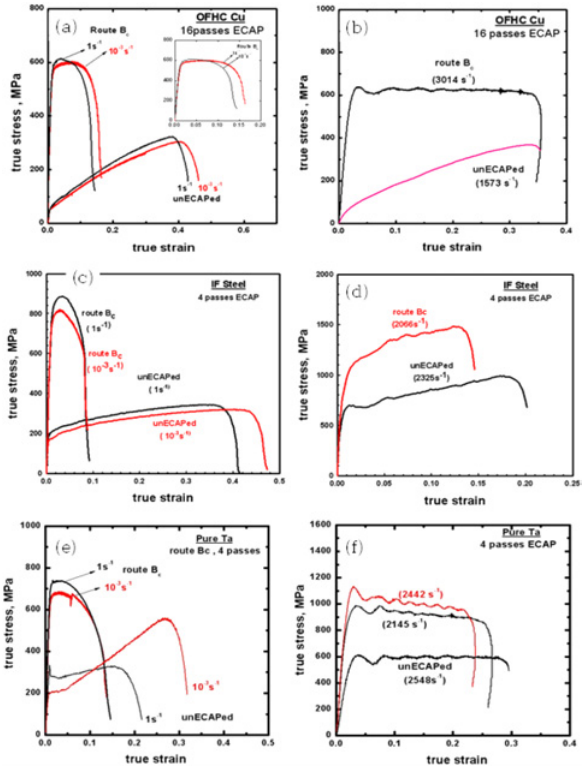

Figure 3. True stress-strain curves of (a) OFHC Cu at static, (b) OFHC Cu at dynamic, (c) IF steel at static, (d) IF Steel at dynamic, (e) Ta at static and (f) Ta at dynamic.

Figure 4. DTE fragments of CG Cu and UFG OFHC Cu in sequence exiting the DTE die. The DTE direction is from left to right.

3.2. Mechanical properties of CG and UFG materials

The true stress-strain curves of CG and UFG sample are shown in Fig. 3. The yield stress of UFG materials were increased a few ten times that of CG materials. Meanwhile, the elongation of UFG materials were decreased a few times that of CG materials. As usual, regardless of the strain rate, CG Cu and IF steel exhibited extensive strain hardening after low stress yielding while near-perfect plasticity without strain hardening after high stress yielding occurred in UFG Cu and Ta. While UFG IF steel showed strain hardening at high strain rate test (∼2000/s) with SHPB.

3.3. DTE behaviour: Fragmentation, ductility

The representative soft-recovered fragments of the CG Cu and UFG Cu after DTE are shown in Fig. 4: the conical fragment is the remnants remained in the DTE die. For all three runs of each sample, the CG Cu was fragmented

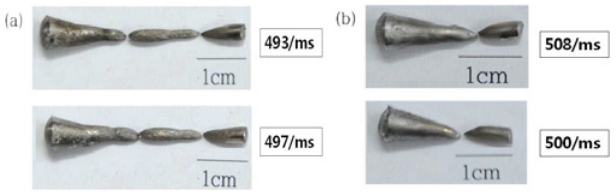

Figure 5. DTE fragments of (a) CG IF steel and (b) UFG IF steel in sequence exiting the DTE die.

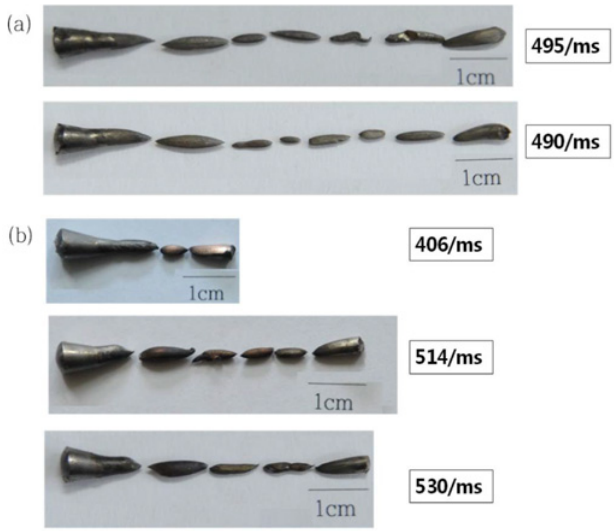

Figure 6. DTE fragments of CG and UFG pure Ta in sequence exiting the DTE die.

into 4 pieces while the UFG Cu was fragmented into 3 pieces. All fragments except the conical remnants were in the lenticular shape indicating that fragmentation occurred by plastic instability (i.e. necking) rather than void coalescence.

The average DTE ductility of each sample were 45.09 mm (∼592%) and 33.331 mm (∼437%) for the CG and UFG Cu, respectively: the DTE ductility is the sum of the axial ductility of each fragment with respect to the initial sample diameter, i.e. DTE ductility $= (Sd_i - d_o)/d_o$ where d_i is the longitudinal length of the i^{th} fragment and d_o is the initial sample diameter. The soft-recovered fragments of the CG and UFG IF Steel after DTE are shown in Fig. 5: the conical fragment is the remnants remained in the DTE die. For all two runs of each sample, the CG IF steel was fragmented into 3 pieces while the UFG IF Steel was fragmented into 1 piece. All fragments except the conical remnants were in the lenticular shape similar to OFHC Cu. The DTE ductility of each sample was 41.31 mm (542%), 41.31mm (518.8%) and 23.22 mm (∼305%), 23.16 mm (∼304%) for the CG and UFG IF steel, respectively.

The recovered fragments of the CG and UFG pure Ta after DTE are shown in Fig. 6. The CG tantalums were fragmented into 6 or 7 pieces while the UFG tantalums were fragmented into 4 or 5 piece. All fragments except the conical remnants were in the lenticular shape similar to the other above samples. The DTE ductility of each sample was 70.71 mm (∼930%), 72.2 mm (∼947.5%) for the CG

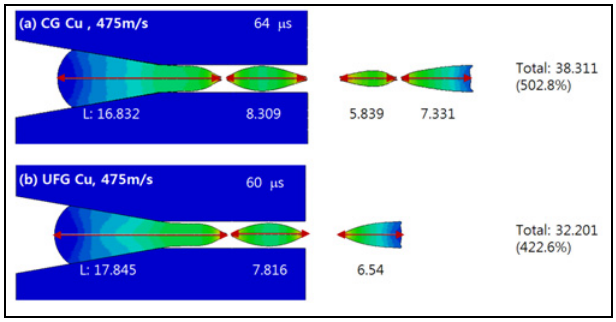

Figure 7. FEM simulation result showing the fragmentation of the DTE fragment of (a) CG Cu, and (b) UFG Cu.

and 33.51 mm (∼440%), 51.82 mm (680.05%), 49.35 mm (∼647.6%) % for the UFG tantalums, respectively.

3.4. Numerical simulation results

The present DTE behavior of CG and UFG OFHC Cu was numerically simlulated by the LS-DYNA FEM code with the 2D R-adaptivity remeshing. A simulation example for strain after complete fragmentation at ∼60 μsec is presented in Fig. 7. The number of fragment is correctly prediced by simulation, i.e. 4 fragments for CG Cu and 3 fragments for UFG Cu. The simulated total length of CG Cu and UFG Cu was 38.3 mm (DTE elongation ∼503%) and 32.2 mm (DTE elongation ∼423%), respectively. The simulated DTE elonagtion of UFG Cu is in reasonable agreement with the experimental one (∼437%). In contrast, for CG Cu, the experimental DTE elongation (∼592%) was larger than the simulated one (503%). The maximum strain was developed at the necked region in both sample with the similar value. The strain at the necked region upon fragmentation reached ∼5.5. Simulation revealed more localized necking in UFG Cu, possibly causing smaller DTE elongation than CG Cu. In both sample, the strain rate was also maximum at the necked region with $10^5\,s^{-1}$ order which is at least one order or more higher than that achievable by the ordinary Hopkinson test. The maximum strain rate of UFG Cu was slightly higher than that of CG Cu, corresponding to more diffused strain distribution in the latter. The stress imposed by impacting the die was higher in UFG Cu due to its higher yield and flow stresses. The samle velocity was maximum at the exiting tips by the inertia effect. The tip (i.e. maximum) velocity of CG Cu was faster than that of UFG Cu. As expected considerable temperature rise occurred by adiabatic heating. Temperature at the stretched portion in the straight channel was close to or even higher than 700 °K which is about 0.5 T_m. It was locally over 800 °K (∼0.6 T_m of Cu) upon fragmentation.

A simulation example DTE behavior of CG and UFG IF steeels were shown in Fig. 8. The number of fragment is correctly prediced by simulation, i.e. 3 fragments for CG steel and 2 fragments for UFG steel. The simulated total length of CG steel and UFG steel was 34.92 mm (DTE elongation ∼458%) and 27.17 mm (DTE elongation ∼357% respectively. The simulated DTE elonagtion of CG and UFG steel is in reasonably well agreement with the experimental one ∼519% for CG and ∼304% for UFG.

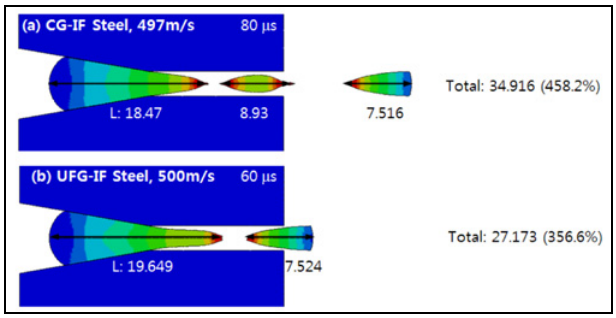

Figure 8. FEM simulation result showing the fragmentation of the DTE fragment of (a) CG IF steel, and (b) UFG IF steel.

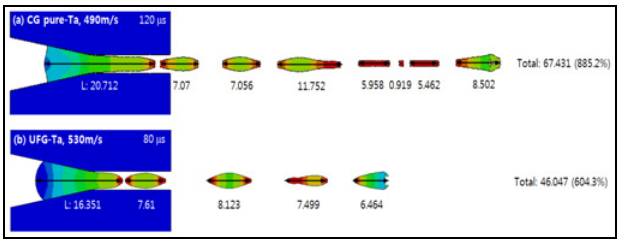

Figure 9. FEM simulation result showing the fragmentation of the DTE fragment of (a) CG Ta, and (b) UFG Ta.

A simulation example DTE behavior of CG and UFG pure tantalums were shown in Fig. 9. The number of fragment is correctly prediced by simulation, 7 fragments for CG tantalum and 5 fragments for UFG steel. The simulated total length of CG tantalum and UFG tantalums was 67.43 mm (DTE elongation ∼885%) and 46.05 mm (DTE elongation ∼604%), respectively. The simulated DTE elonagtion of CG and UFG tantalums are in reasonably good agreement with the experimental one (∼948%) for CG and (∼648%) for UFG tantalum repectively.

4. Summary

1. A series of dynamic tensile extrusion (DTE) tests, the newly developed mechanical test at high strain rate, was conducted on coarse grained (CG) and ultrafine grained (UFG) OFHC Cu, IF steel, and pure Ta. CG materials exhibited higher DTE elongation than UFG materials.
2. The inferior metal jet stability of UFG materials are caused by its initial higher strength and lack of strain hardenability compared to CG materials.
3. Numerical simulation empoying the mesh adaptivity predicted the fragmentation behavior of CG and UFG materials in terms of DTE elonagtion and the number of fragments. The results of numerical simulation are in reasonsably well agreement with the those of experimental.

References

[1] Gray III G.T. et al. 2006 *Shock Compression of Condense Matter* ed by Furnish M.D. et al. (American Institute of Physics) p. 725
[2] Cao F. et al. 2008 *Acta Mater*. **56**, 5804
[3] Escobedo J.P. et al. 2012 *Acta Mater*. **60**, 4379
[4] Farrokh B. and Kahn A.S. 2009 *Int. J. Plasticity* **25**, 715
[5] Q. Wei, T. Jiao, K.T. Ramesh and E. Ma, Scripta Mater. **50**, 359 (2004)
[6] D.H. Shin, D.Y. Hwang, Y.J. Oh, K.-T. Park, Metall. Mater. Trans. A **35A**, 825 (2004)
[7] A.H. Chokshi, M.A. Meyers, Scripta Metall. Mater. **24**, 605 (1990)
[8] Park K.T. et al. 2013 Mater SciEng A **569**, 61
[9] LS-DYNA® *Keyword User's Manual*, 2007 Vol. 1. Version 97 (Livermore Software Technology Corp)